Cell Reports, Volume *29*

Supplemental Information

Polymorphic Immune Mechanisms Regulate Commensal Repertoire

Aly A. Khan, Leonid Yurkovetskiy, Kelly O'Grady, Joseph M. Pickard, Renée de Pooter, Dionysios A. Antonopoulos, Tatyana Golovkina, and Alexander Chervonsky

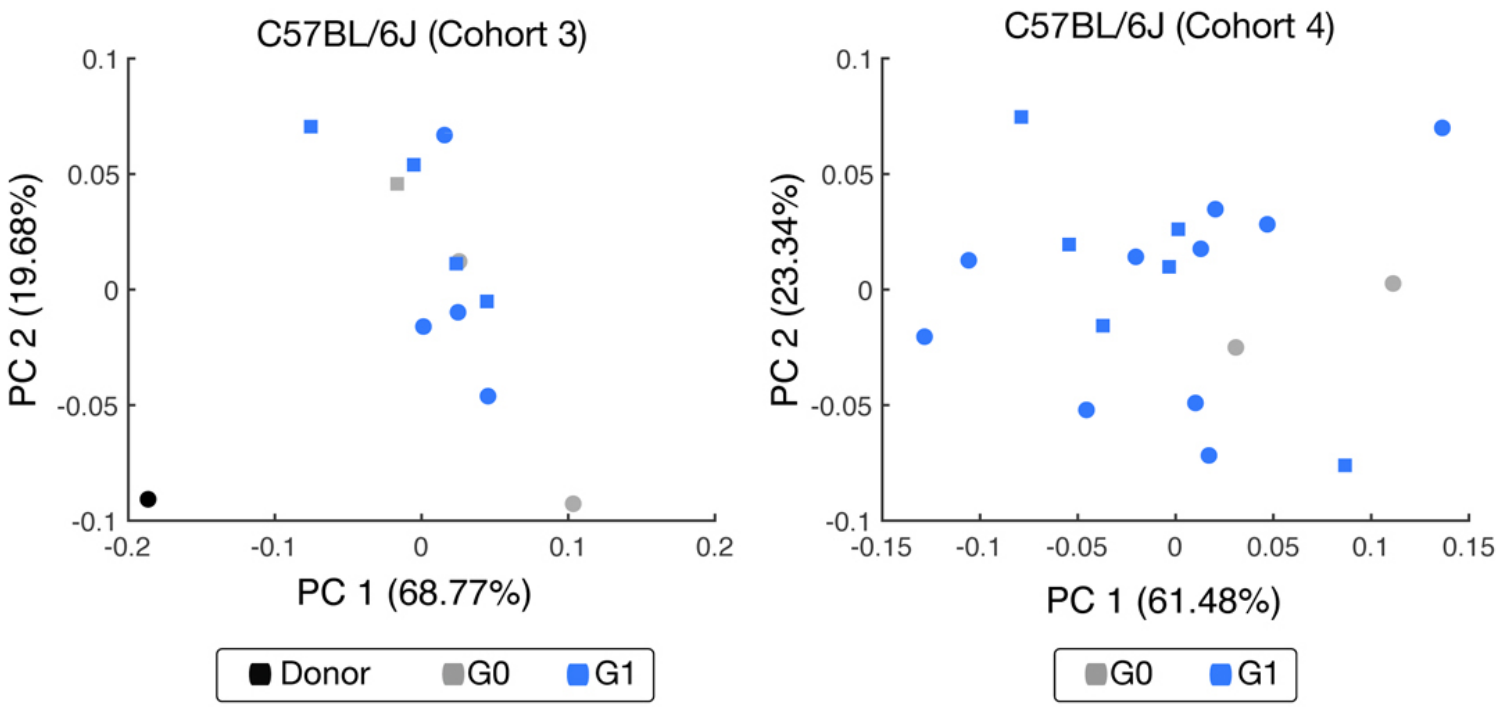

Figure S1. **PCA showing that G0 microbiomes are not separable from G1 in two independent experiments. Related to Figure 1**. Donor - B6 microbiota. Circles, females; squares, males.

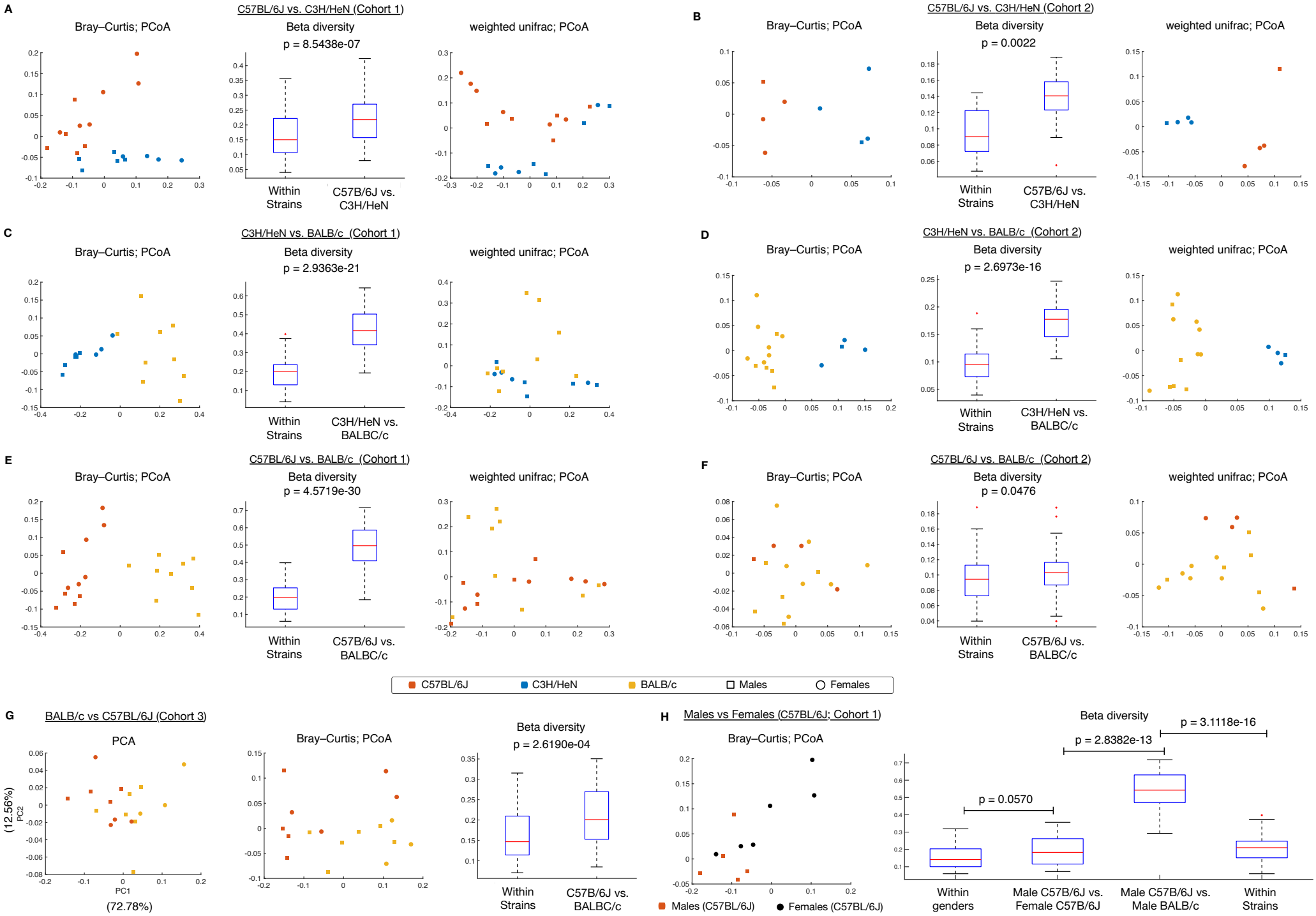
A
C57BL/6J vs. C3H/HeN (Cohort 1)
Bray–Curtis; PCoA
Beta diversity
p = 8.5438e-07
weighted unifrac; PCoA
Within Strains
C57B/6J vs. C3H/HeN
B
C57BL/6J vs. C3H/HeN (Cohort 2)
Bray–Curtis; PCoA
Beta diversity
p = 0.0022
weighted unifrac; PCoA
Within Strains
C57B/6J vs. C3H/HeN
C
C3H/HeN vs. BALB/c (Cohort 1)
Bray–Curtis; PCoA
Beta diversity
p = 2.9363e-21
weighted unifrac; PCoA
Within Strains
C3H/HeN vs. BALBC/c
D
C3H/HeN vs. BALB/c (Cohort 2)
Bray–Curtis; PCoA
Beta diversity
p = 2.6973e-16
weighted unifrac; PCoA
Within Strains
C3H/HeN vs. BALBC/c
E
C57BL/6J vs. BALB/c (Cohort 1)
Bray–Curtis; PCoA
Beta diversity
p = 4.5719e-30
weighted unifrac; PCoA
Within Strains
C57B/6J vs. BALBC/c
F
C57BL/6J vs. BALB/c (Cohort 2)
Bray–Curtis; PCoA
Beta diversity
p = 0.0476
weighted unifrac; PCoA
Within Strains
C57B/6J vs. BALBC/c
C57BL/6J
C3H/HeN
BALB/c
Males
Females
G
BALB/c vs C57BL/6J (Cohort 3)
PCA
(12.56%) PC2
PC1 (72.78%)
Bray–Curtis; PCoA
Beta diversity
p = 2.6190e-04
Within Strains
C57B/6J vs. BALBC/c
H
Males vs Females (C57BL/6J; Cohort 1)
Bray–Curtis; PCoA
Males (C57BL/6J)
Females (C57BL/6J)
Beta diversity
p = 3.1118e-16
p = 2.8382e-13
p = 0.0570
Within genders
Male C57B/6J vs. Female C57B/6J
Male C57B/6J vs. Male BALB/c
Within Strains

Figure S2. Principal coordinate analysis (PCoA) and comparison of β diversity between various strains colonized with C57BL/6J microbiota. Related to Figure 2.
A-F. PCoA was performed using Bray–Curtis distance (left) and Weighted UniFrac distance (right), demonstrating reproducible separation of strains using two different distance metrics; a non-phylogenetic based metric (Bray–Curtis) and a phylogenetic based metric (Weighted UniFrac).
One-sided non-parametric Wilcoxon rank sum test was used to determine if the β diversity estimated using Bray-Curtis distance metric between strains was greater than differences within a strain. The following comparisons are shown: C57BL/6J vs. C3H/HeN (Cohort 1) (**A**); C57BL/6J vs. C3H/HeN (Cohort 2)(**B**); C3H/HeN vs. BALB/c (Cohort 1) (**C**); C3H/HeN vs. BALB/c (Cohort 2) (**D**);C57BL/6J vs. BALB/c (Cohort 1) (**E**); C57BL/6J vs. BALB/c (Cohort 2) (**F**).
G. Comparison of the microbiomes of two ex-GF strains (BALB/c vs C57BL/6J) colonized with the same microbiotas from Cohort 3 shown as PCA (left), PCoA using Bray–Curtis distance (center), and β diversity estimated using Bray-Curtis distance metric between strains (right).
H. Comparison of the microbiomes of male and female ex-GF C57BL/6J mice from Cohort 1 shown as PCoA using Bray–Curtis distance. Males are represented by red rectangles, females by black circles (left). One-sided non-parametric Wilcoxon rank sum tests were used to examine if strain differences are greater than gender differences (right). β diversity found between male C57B/6J and female C57B/6J mice showed a strong trend for being greater than β diversity found within gender among C57B/6J mice ($p = 0.0570$). The β diversity found between male C57B/6J and male BALB/c mice was significantly greater than β diversity found between male C57B/6J and female C57B/6J ($p = 2.8382e-13$). The β diversity found between male C57B/6J and male BALB/c mice is significantly greater than β diversity found among male mice within strains ($p = 3.1118e-16$).

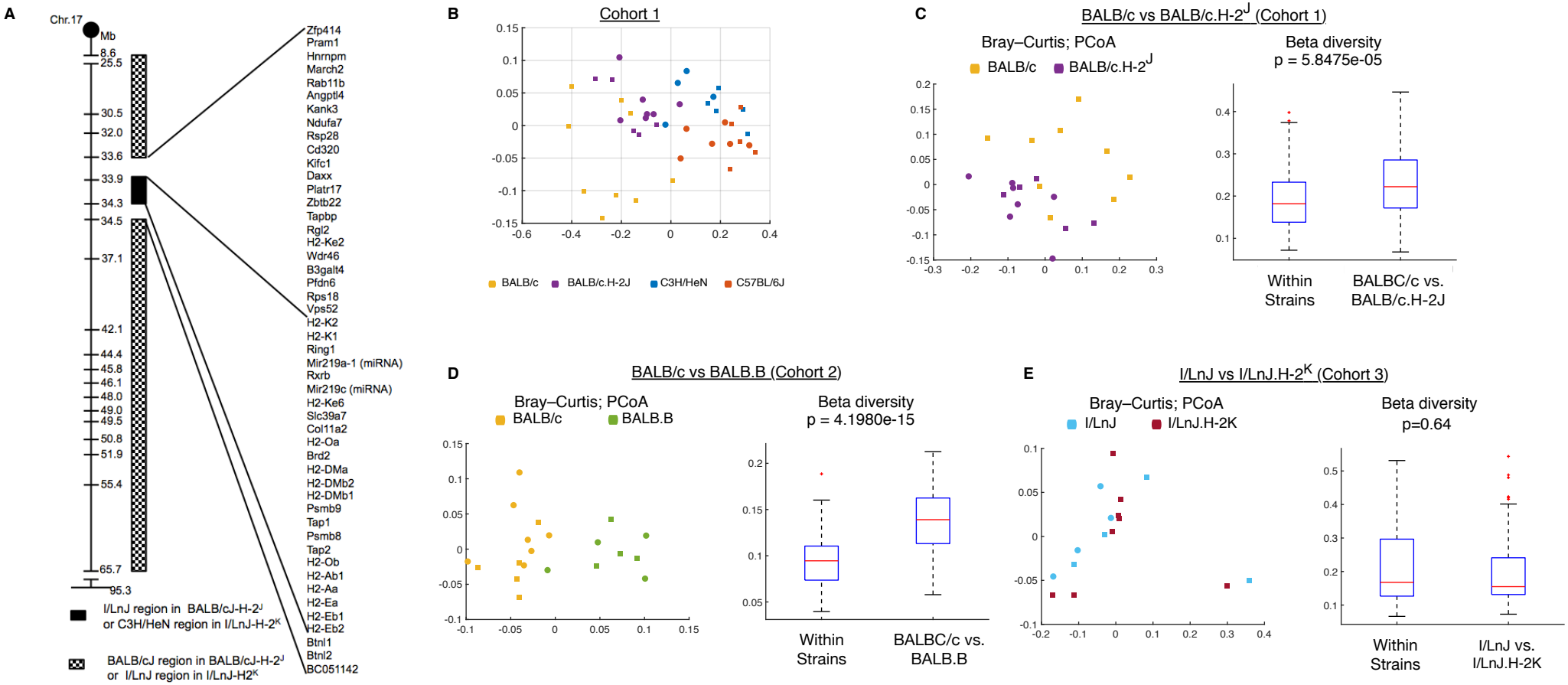

Figure S3. Additional analyses of microbiomes of MHC-congenic strains of mice. Related to Figure 3.

A. Schematic map of the congenic BALB/cJ line containing the MHC locus from I/LnJ mice and I/LnJ mice containing the MHC locus from C3H/HeN mice. The replacement was achieved by crossing the two strains followed by multiple back-crossings to BALB/cJ mice and I/LnJ mice respectively. At generation N10 mice in both back-crosses were intercrossed. Open areas upstream and downstream on the the MHC locus - regions of undefined origin.

B. 2-D PCA analysis of the microbiomes of BALB/cJ (yellow), BALB/c-H-2j (magenta), C3H/HeN (blue) and C57BL/6J (red) mice. Dots – females, squares – males. 3-D plot of the same data analysis is shown in Figure 3A.

C-E. Principal coordinate analysis (PCoA) visualizations and comparison of β diversity between various strains colonized with C57BL/6J microbiota. PCoA performed using Bray–Curtis distance (left) and one-sided non-parametric Wilcoxon rank sum tests used to examine if strain differences are greater than gender differences (right): BALB/c vs BALB/c.H-2J (Cohort 1) (**C**); BALB/c vs BALB.B (Cohort 2) (**D**); I/LnJ vs I/LnJ.H-2K (Cohort 3) (**E**).

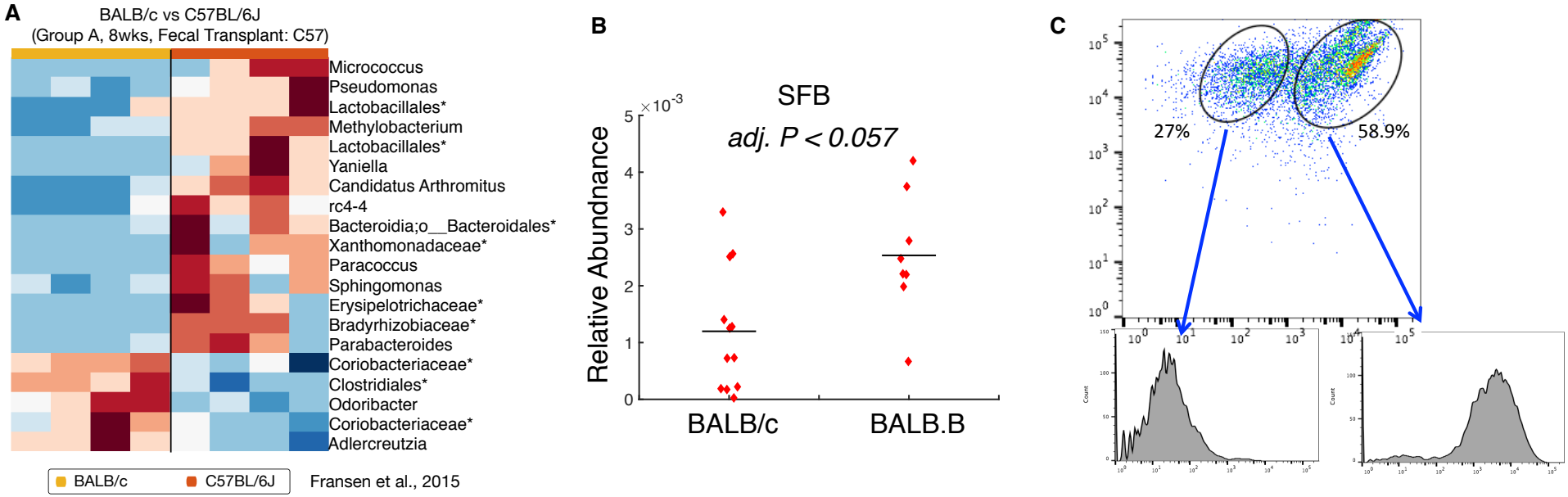

Figure S4. **Additional analyses of the microbiomes. Related to Figure 3**

A. Data from Fransen et al., 2015 reanalyzed. Heat map showing statistically significant lineage differences ($P < .05$, FDR adjusted t-test) of bacterial lineages between ex-GF BALB/c vs. C57BL/6J 8 weeks after fecal transplant with B6 microbiota. Notably, *Candidatus Arthromitus* (SFB) was higher in C57BL/6J.

B. Relative abundance of SFB bacteria in BALB/cJ (H-2^d) and BALB.B (H-2^b) mice from our high throughput sequencing experiment (Cohort 3).

C. An example of sorting of colonic bacteria for IgA-seq experiments. Colonic contents free of debris was stained with anti-IgA antibodies conjugated to the APC fluorochrome and sorted into + and - populations, which were reanalyzed before extracting DNA for sequencing.

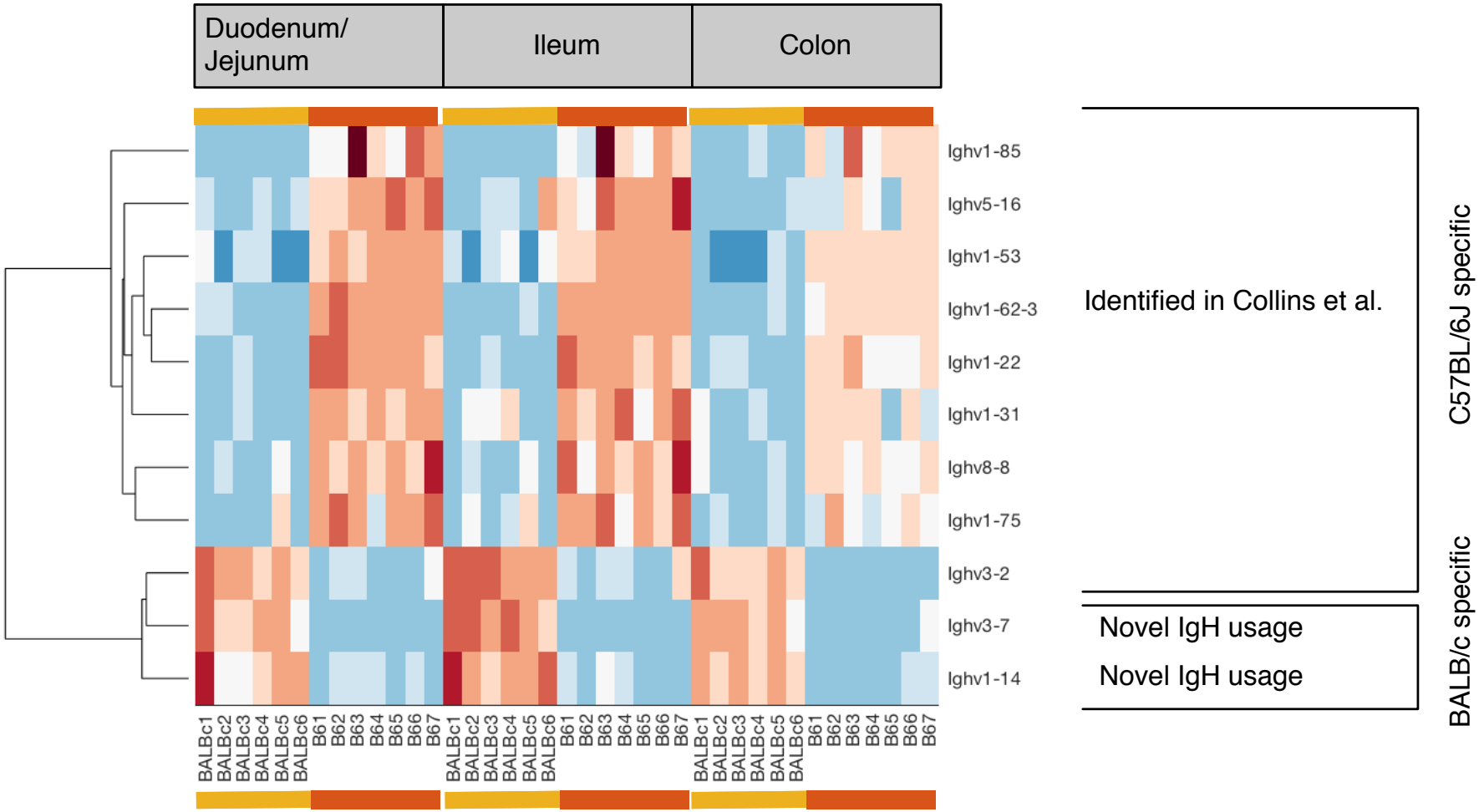

Figure S5. BALB/cJ and C57BL/6J mice utilize different families of the variable regions of the heavy chain of immunoglobulins. Related to Figure 4. Some of these differences were reported before (Collins et al, 2015), some are reported here.

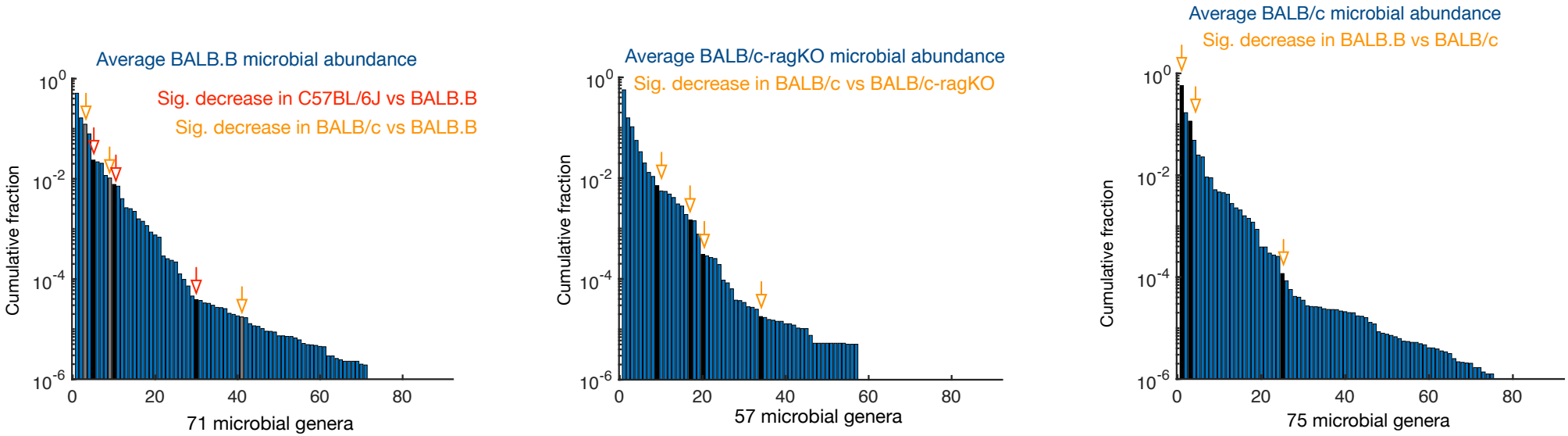

Figure S6. **Limited number of bacterial lineages is controlled by polymorphic innate and adaptive mechanisms. Related to Figure 3**. Arrows show abundances of bacterial lineages significantly different between indicated strains of mice. Abundance itself was not a factor for controlling mechanisms – lineages with higher and very low abundances were selectively controlled.

Table S1. Input microbiota, cohort structure and mouse numbers in the current study. Related to Figures 1-4.

Cohort	Source of microbiota	G0 strains		G1 F	G1 M	Total number of mice per group per experiment
1	B6 UC (JAX)	B6	1F	2	1	**11**
		B6	1F	4	4	
		BALB/cJ	1F	0	10	**10**
		BALB.H-2^{j}	1F	7	5	**12**
		C3H/HeN	1F	4	5	**9**
2	B6 TAC	BALB/cJ Rag1$^{-/-}$	1F	1	2	**5**
		BALB/cJ Rag1$^{-/-}$	1F	1	1	
		C57BL/6J	1F	1	1	**4**
		C57BL/6J	1F	2	0	
		BALB.H-2^{j}	1F	0	4	**7**
		BALB.H-2^{j}	1F	3	0	
		BALB/cJ	1F	2	3	**12**
		BALB/cJ	1F	5	2	
		I/LnJ	1F	1	2	**12**
		I/LnJ	1F	1	4	
		I/LnJ	1F	2	2	
		C3H/HeN	1F	1	1	**4**
		C3H/HeN	1F	2	0	
		BALB.H-2^{b}	1F	2	2	**8**
		BALB.H-2^{b}	1F	2	2	
3	B6 TAC	I/LnJ.H-2^{k}	1F	0	4	**8**
		I/LnJ.H-2^{k}	1F	0	4	
		BALB/cJ	1F	2	4	**10**

		BALB/cJ	1F	1 3	
		I/LnJ	1F	2 3	**8**
		I/LnJ	1F	2 1	
		B6	1F	2 2	**8**
		B6	1F	2 2	
4	B6 JAX	B6	1F	3 2	**16**
		B6	1F	2 2	
		B6	1F	5 2	

Sources of microbiota for GF mice repopulation: Cohort 1 - B6 (UC) JAX originated from The Jackson Laboratory, but were bred and housed at the University of Chicago for several generations; Cohorts 2 and 3 – donors arrived straight from Taconic; B6 JAX – donors arrived straight from The Jackson Laboratory.

Each line shows the size and gender break of the progeny of a particular G0 female.

Last column summarizes mouse numbers used for statistical analysis in each experiment (cohort).

Table S2. Selected genes with differential expression in BALB/c and B6 gut chosen by relevant gene ontology (GO) category and relevance to immunity and/or inflammatory conditions in the gut. Related to Figure 4.

Physiological function Gene name	GO ID	GO process association	Association with immunity and disease	References
Complement activation *C1rb* *C1s2*	 0006956 0006956	 Complement activation Complement activation		
Mucosal pentraxins *Mptx1* *Mptx2*			Microbial dysbiosis Antimicrobial peptide expressing Paneth cells	(van der Meer-van Kraaij et al., 2007) (Haber et al., 2017)
Inactivators of xenobiotics and toxins *Ces1b* *Fmo4* *Gsta1*	 0016042 0055114 0006749	 Lipid catabolic process TMAO inactivation Glutathione metabolism	Enzymatic hydrolysis Gut microbiota cardio-vascular disease	(Hosokawa, 2008) (Wang et al., 2011)
NK cell differentiation and activation *H60c* *Il11ra2* *Raet1e*	 0001913 0004896 0001913	 Cell mediated cytotoxicity Cytokine receptor activity Cell mediated cytotoxicity		
Glycosyltransferases *St3gal4*	0006486	Protein glycosylation	Intestinal inflammation and microbial dysbiosis	(Huang et al., 2015)
Trim proteins – regulators of inflammation and anti-viral immunity *Trim30d* *Trim34b* *Trim80*			Innate immunity and pathogen recognition	(Ozato et al., 2008) (Ozato et al., 2008) (Ozato et al., 2008)
Gasdermins *Gsdmc3* *Gsdms4*	 0012501 0012501	 Programmed cell death Programmed cell death	 Inflammatory bowel disease Inflammatory bowel disease	 (Yuan et al., 2018) (Yuan et al., 2018)

Reactive oxygen species production/Oxidation of microbial metabolites *Duox1*	0019221	Cytokine-mediated signaling pathway	Gastric colonization by *H. Felis*	(Grasberger et al., 2013)
Neutrophil function *Prg2* *Padi4* *Tmem116*	0002376 0002376	Immune system process Immune system process	Crohn's disease Septic shock mortality	(Han et al., 2013) (Costa et al., 2018)
Intestinal barrier function *Afm* *Tjap1* *Pianp*	0008431 0005923 0050776	Vitamin E binding Bicellular tight junction	Intestinal homeostasis	(Mihara et al., 2016)
Peptidase inhibitors *Serpina10* *Serpina1a* *Serpina1b* *Serpina3a* *Serpina3h*	0010466 0010466 0010466	Negative regulation of peptidase activity Negative regulation of peptidase activity Negative regulation of peptidase activity		
Interferon-induced genes *Ifi44l* *Ifi202b* *Gvin1*	0006955 0045087	Immune response Innate immune response	Microbial diversity correlated with expression of these genes Immunity to intracellular pathogens	(Brodziak et al., 2013) (MacMicking, 2004)
Inflammasome regulation *Nlrp1b*	0045087	Innate immune response	Colitis	(Williams et al., 2015)
Macrophage phagocytic function *Spp1*	0006954	Inflammatory response		(Toyonaga et al., 2015)
Metabolic genes *Eno1b* (retrotransposed)			*H. Pylori*-mediated gastric diseases	(Chen et al., 2014)

Table S3. **Complete list of genes with significant difference in expression between BALB/c and B6 gut. Related to Fig.4**. Variable regions of immunoglobulin genes are shown separately. DJ-duodenum/jejunum.

Host Genes			Immunoglobulin Genes		
Duodenum/Jejunum	**Ileum**	**Colon**	**IG-DJ**	**IG-Ileum**	**IG-Colon**
1700011H14Rik	1700011H14Rik	2010005H15Rik	Ighv1-14	Ighv1-13	Ighv1-14
2200002J24Rik	2200002J24Rik	5830417I10Rik	Ighv1-15	Ighv1-14	Ighv1-15
5830417I10Rik	5830417I10Rik	9530053A07Rik	Ighv1-22	Ighv1-15	Ighv1-2
9530053A07Rik	9530053A07Rik	Actc1	Ighv1-31	Ighv1-22	Ighv1-20
Acta1	A930018M24Rik	Afm	Ighv1-39	Ighv1-23	Ighv1-22
Actc1	Acta1	AK157302	Ighv1-53	Ighv1-27	Ighv1-23
AK157302	Actc1	Apoa2	Ighv1-56	Ighv1-31	Ighv1-25
BC035947	AK157302	Atp8b5	Ighv1-58	Ighv1-36	Ighv1-27
Camk2b	Akt2-ps	BC025446	Ighv1-62	Ighv1-38	Ighv1-30
Clec2j	Apoa2	C1rb	Ighv1-62-2	Ighv1-43	Ighv1-31
Cyp2c29	BC035947	C1s2	Ighv1-62-3	Ighv1-53	Ighv1-33
Cyp2c67	C1rb	Cib3	Ighv1-71	Ighv1-58	Ighv1-36
Cyp3a59	C1s2	Col4a6	Ighv1-75	Ighv1-62	Ighv1-37
Defa-ps18	Ces1b	Cyp2c67	Ighv1-76	Ighv1-62-2	Ighv1-43
Defa2	Clec2j	Cyp2r1	Ighv1-78	Ighv1-62-3	Ighv1-53
Defa20	Col4a6	Dynlt1a	Ighv1-81	Ighv1-71	Ighv1-62-3
Defa21	Cyp2c67	Ear-ps3	Ighv1-84	Ighv1-75	Ighv1-67
Defa22	Cyp3a44	Eno1b	Ighv1-85	Ighv1-84	Ighv1-75
Defa26	Defa-ps18	ENSMUST00000012440.12	Ighv10-3	Ighv1-85	Ighv1-81
Defa27	Defa-ps5	ENSMUST00000160663.1	Ighv14-4	Ighv1-86	Ighv1-83
Defa28	Defa-ps8	Fmo4	Ighv2-9	Ighv2-9	Ighv1-85
Defa32	Defa2	Gbp10	Ighv3-1	Ighv3-1	Ighv1-86
Defa33	Defa20	Gbp2b	Ighv3-2	Ighv3-2	Ighv14-4
Defa35	Defa21	Gvin1	Ighv3-7	Ighv3-7	Ighv2-4
Dynlt1a	Defa22	H2-Ea-ps	Ighv5-16	Ighv4-2	Ighv2-6
Eno1b	Defa26	H2-Q3	Ighv7-2	Ighv5-16	Ighv2-6-8
ENSMUST00000116434.9	Defa27	H60c	Ighv8-8	Ighv7-2	Ighv2-9
Gsdmc3	Defa28	Hist1h2aa	Igkv1-99	Ighv8-11	Ighv3-1
Gsdmc4	Defa32	Hist1h2ao	Igkv4-62	Ighv8-8	Ighv3-2
Gvin1	Defa33	Hmga1-rs1		Igkv7-33	Ighv3-7
H2-Ea-ps	Duox1	I830127L07Rik		Igkv8-31	Ighv4-2
H2-K2	Dynlt1a	Ifi202b			Ighv5-16
Hist1h2aa	Eno1b	Ifi44l			Ighv5-2
Hist3h2bb-ps	ENSMUST00000012440.12	Il11ra2			Ighv6-6
Hmga1-rs1	ENSMUST00000090860.6	Klk15			Ighv6-7
Hmgb1-ps8	Gsdmc4	Lrmda			Ighv7-2
Ifi202b	Gsdmcl2	Marcksl1-ps4			Ighv7-4
Ifi44l	Gsta1	Mptx2			Ighv8-11
Itpa-ps1	Gvin1	Mrpl48-ps			Ighv8-2
Mcoln3	H2-Ea-ps	Mrto4-ps2			Ighv8-8

Mptx1
Mrpl48-ps
Msantd1
Nlrp1b
Nlrp1c-ps
Pnp2
Prg2
Rbpsuh-rs3
Rpl15-ps1
Rpl3-ps1
Rplp0-ps1
Rps12-ps9
Rps3a2
Serpina3a
Skiv2l-ps1
Sprr2a1
Sspo
St3gal4
Sycp1
Tdg-ps
Them7
Tjap1
Tmem116
Tpm3-rs7
Trbv29
Trim34b
Trim80
Vmn1r212
Wsb2-ps

H2-Q3
Hist1h2aa
Hist1h2ao
Hist2h2aa2
Hmga1-rs1
Hmgb1-ps8
I830127L07Rik
Ifi202b
Ifi44l
Il11ra2
Insl3
Mptx1
Mrpl48-ps
Nlrp1b
Nlrp1c-ps
Nr0b2
Nudc-ps1
Pianp
Pik3c2g
Pnp2
Rbpsuh-rs3
Rpl3-ps1
Rpl35a-ps2
Rpl35a-ps3
Rpl35a-ps4
Rpl35a-ps6
Rplp0-ps1
Rps12-ps9
Rps2-ps6
Rps3a2
Serpina10
Serpina3h
Sh2d6
Sh2d7
Skiv2l-ps1
Spp1
Sprr2a1
Sspo
St3gal4
Sycp1
Tdg-ps
Tdpx-ps1
Them7
Tjap1
Tmem116
Tpm3-rs7
Trbv29

Mup-ps23
Nlrp1b
Nxpe4
Nxpe5
Oas2
Padi4
Pkhd1
Pnp2
Raet1e
Rbpsuh-rs3
Rpl3-ps1
Rpl35a-ps2
Rpl35a-ps3
Rpl35a-ps4
Rpl35a-ps6
Rpl36-ps2
Rplp0-ps1
Rps12-ps9
Rps3a2
Serpina1a
Serpina1b
Skiv2l-ps1
Slc22a29
Sycp1
Tdg-ps
Tdpx-ps1
Tpm3-rs7
Trim30c
Trim30d
Trim34b
Unc5a
Wsb2-ps

Igkv1-88
Igkv3-2
Igkv4-50
Igkv4-79
Igkv4-92
Igkv7-33

Trim34b
Trim80
Wsb2-ps